Journal of Solid Mechanics Vol. 11, No. 3 (2019) pp. 678-689
DOI: 10.22034/JSM.2019.666809

Noise Effects on Modal Parameters Extraction of Horizontal Tailplane by Singular Value Decomposition Method Based on Output Only Modal Analysis

P. Jalali, S. Varahram, R. Hassannejad *, M.H. Sadeghi

Vibration and Modal Analysis Research Lab, Faculty of Mechanical Engineering, University of Tabriz, Tabriz, Iran

Received 29 June 2019; accepted 30 August 2019

ABSTRACT

According to the great importance of safety in aerospace industries, identification of dynamic parameters of related equipment by experimental tests in operating conditions has been in focus. Due to the existence of noise sources in these conditions the probability of fault occurrence may increases. This study investigates the effects of noise in the process of modal parameters identification by Output only Modal Analysis (OMA) method using Singular Value Decomposition (SVD) algorithm. The study case is the horizontal tailplane of the aircraft; therefore, at first, the modal parameters of the tailplane are obtained numerically. Then a cantilever beam is used to perform experimental tests with regard to the high aspect ratio of the modeled tailplane. The modal parameters of the beam are obtained nonparametrically by Experimental Modal Analysis (EMA) and OMA. In order to investigate the effects of noise in a controlled manner, the artificial excitation namely the shaker with the random force is used. Then, the effects of noisy measurements on the specifications of the system in EMA and OMA methods are investigated. The results indicate that: 1. The OMA method has more resistance against the noise for extracting natural frequencies. 2. The results of the Modal Assurance Criterion (MAC) values by EMA method, in the condition of noise existence in output data, are worse than the noise existence in input data. 3. The average of MAC values in general condition of EMA method by noisy input & output data is worse than the OMA method.

Keywords: Output only modal analysis; Frequency domain decomposition; Finite element; Singular value; Noise measurement.

1 INTRODUCTION

IN today's industrialized world, optimum designing of the complex mechanical, civil or urban spatial structures is very important. The design procedures must meet the mechanical and civil engineering requirements so that the

*Corresponding author.
E-mail address: hassannejhad@tabrizu.ac.ir (R.Hassannejad).

final constructed structures have high strength and elasticity, and low weight [1]. Dynamic analysis is one of the main requirements for structural design, repair, and maintenance of structures; in this respect, different methods and approaches have been developed at various levels to investigate the smallest effects on the above-mentioned systems, even at nanoscale levels [2-9]. One of the most fundamental sections of dynamic analysis is the determination of the dynamic characteristics of the structures. The modal analysis methods are powerful tools to achieve this purpose, which are divided into two categories of experimental modal analysis and output only modal analysis. According to the importance of aviation and aircraft structural safety, many researchers focused on this subject and performed many studies regarding the modal parameters extraction [10]. Neu et al. studied the influence of the attack angle and the wind velocity on the modal parameters of a composite cantilever by using the OMA [11]. In another research they used different methods to extract the modal characteristics of a wing, which was excited by transonic flow in a wind tunnel; the results indicated that the stochastic subspace identification (SSI) algorithm has an excellent identification capability [12]. They also proposed a new algorithm in OMA that can be effective to identify the dynamic parameters of highly damped structures, as well as the low signal to noise ratio situations [13]. Jelicic et al. monitored the frequencies and damping ratios during a flight test via OMA by using the SSI and Least-square complex frequency domain (LSCF) algorithms to extract the modal parameters [14]. Jia et al. conducted numerical simulation and experimental modal test on the deployable-retractable wing to identify the modal parameters using LMS PolyMAX solver [15]. Moaveni et al. investigated the uncertainty in three methods of OMA under the different conditions of uncertainty sources; the results indicated that the amplitude of stimulation has the most influence on modal parameters identification, especially on the natural frequencies [16]. Mellinger et al. developed a new method based on the variance approach to computing the uncertainty of modal parameters, which are identified by four different modal analysis methods consist of output only, input-output, data-driven, and covariance driven algorithms [17].

However, despite all the improvements in modal analysis methods (both the EMA and the OMA), existence of noise in the measured data have been a great disturbance and limiting factor, which may cause some errors and inaccuracy of the results; this problem has prompted researchers to investigate the various aspects of noise, and eliminate its effects. One assumption in this regard is that the characteristics of the measurement noise are already known, such as the variance and the mean value; then the maximum likelihood method can be used to optimize the results [18]. In another technique, it is assumed that the level of noise is limited, and then the transfer function can be approximated by using the Markov parameters [19]. Bai and Raman estimated the real and imaginary parts of the transfer function separately instead of the magnitude and phase; as a result, they proposed a noise-resistant algorithm [20]. Other techniques were also provided, which are based on the estimation of measurement noise and using them to approximate the transfer function [21]. Schoukens et al. compared the performance of Taylor approximation with the Coherence approximation to provide a nonparametric noise model, in order to eliminate the output measurement noise of a linear dynamic system. The results indicated that the Taylor approximation can eliminate the leakage errors better than the Coherence approximation [22]. In another research, they proposed a nonparametric model for output measurement noise from the raw data. They succeeded in eliminating the transient portion because of their smooth treatment [23]. Schoukens et al. demonstrated that the frequency and time domain identifications present equivalent results for the finite data records in the standard conditions; they discussed the non-parametric noise models and explained that such models simplify the identification process in parametric plant models [24]. Juang and Pappa investigated the effects of noise on the process of modal parameters identification by using the eigensystem realization method. They utilized the singular values and modal amplitude coherence to discriminate the noise from the information of the system [25]. Li et al. expressed that the singular value decomposition (SVD) method is one of the best techniques for estimating the modal parameters from the noisy data, which can be used in order to separate the noise from the information of the system [26]. Dorvash and Pakzad introduced the important parameters which can affect the modal identification process and their effects on the accuracy of the results; they also identified the modal parameters of the Golden Gate Bridge by the data which were acquired by wireless sensors and investigated the accuracy of the results by the introduced parameters [27]. Brinker et al. proposed the Frequency Domain Decomposition (FDD) method to identify the modal parameters of a system, which is an OMA method and uses the SVD of the power spectral density (PSD) of the acquired data from the system; they expressed that the FDD method is able to identify the modal parameters from the data which its properties are similar to the white Gaussian noise [28]. This method has been developed and now is one of the conventional OMA methods [29].

As comprehensively explained above, several studies have performed in order to identify the modal parameters of aerospace equipment and structures, and also the problem of the noise existence in the measurement data has considered by researchers and scientists, which eventually resulted in some methods of noise elimination and mathematical noise models; but the great effects of noise in the process of system identification is a critical issue in aerospace industries and aviation safety. One of the main structural components of aircrafts is their horizontal

tailplane, which controls the stability of the aircrafts; accordingly, this paper investigates the effects of the measurement noise in the process of modal parameters identification of the horizontal tailplane of aircrafts, and different conditions of measurement noise in the EMA and OMA are considered and compared with each other. For this purpose, at first the tailplane is modeled and its modal parameters are obtained numerically. To perform the experimental tests, a cantilever beam is used with regard to the high aspect ratio of the modeled tailplane, and the modal parameters of the beam are obtained by EMA (rational fraction polynomial method) and OMA (singular value decomposition algorithm); the results of tests are compared with the results of theoretical and numerical methods, which confirmed that the tailplane can be simplified and modeled by the beam; then 15% random noise is added to the signals which were acquired by tests, and the effects of noisy measurement data on the specifications of system in EMA and OMA methods are investigated and compared with each other.

2 NUMERICAL MODELING OF THE TAILPLANE

Three-dimensional finite element model of the tailplane with details of its skeleton is designed by commercial software. By taking advantage of this model, it is possible to extract the modal parameters of the system. The model of tailplane is presented in Fig. 1.

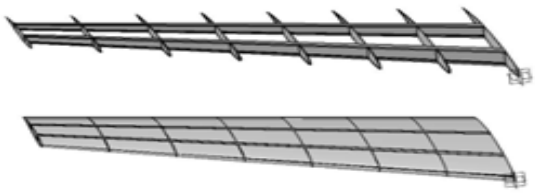

Fig.1
Finite element model of the horizontal tailplane of an aircraft.

Considering that the system will be simulated experimentally by a cantilever beam, the model of the system scaled to two sizes, namely the actual size of the tailplane and the laboratory size of the cantilever beam. Mechanical characteristics of the tailplane which is made by aluminum are presented in Table 1.

Table 1
Mechanical characteristics of the tailplane [30]

Parts involved	Density (Kg/m^3)	Young's modulus (GPa)	Poisson's ratio
shell	2800	70	0.33
rib	2800	70	0.33
beam	2800	70	0.33

After analyzing the system, the first three natural frequencies of the actual size and the laboratory size of the model are presented in Table 2.

Table 2
Natural frequencies of the tailplane which are obtained by numerical method.

	First mode (Hz)	Second mode (Hz)	Third mode (Hz)
Actual size of the tailplane	14.12	56.45	116.4
Scaled size of the tailplane	65.1	293.8	720.12

The first three mode shapes of the tailplane related to its first three natural frequencies are presented in Fig. 2. It should be noted that the mode shapes of the actual size of the model are similar to the laboratory size.

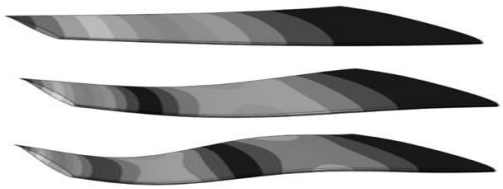

Fig.2
First three mode shapes of the tailplane which are obtained by numerical method.

3 MATERIAL AND METHODS

The first step in the nonparametric methods of EMA is obtaining the frequency response function (FRF), which can be achieved by applying specific input excitation signals to the system and measuring the output response signals, and then post-processing the acquired data.

In order to stimulate the all vibrational modes of a system, a specific excitation force should be used, which involves all the frequencies of the desired frequency range. For this purpose, and in order to simulate the noise and investigate its effects, the random force is used in this study; on the other hand, researchers have shown that the correlation function of random and noisy data can improve the accuracy of the results instead of using the data itself [31]. The correlation function shows the similarity between the signals in specific time periods; the correlation of a random wave has a small amount at each moment because the signal is changing at any moment with regard to its nature. The relation between the input and output random signals in the time domain can be represented as [32]:

$$R_{yy}(\tau) = h(t) * R_{xx}(\tau) \tag{1}$$

In this equation the asterisk (*) indicates the convolution of $h(t)$ and $R_{xx}(\tau)$, the $h(t)$ is the response function in the time domain, $R_{xx}(\tau)$ and $R_{yy}(\tau)$ are autocorrelation of the input and the output signals respectively, and are represented by following relations:

$$R_{xx}(\tau) = E\left(x(t) - x(t+\tau)\right) \tag{2}$$

$$R_{yy}(\tau) = E\left(y(t) - y(t+\tau)\right) \tag{3}$$

Eq. (1) can be converted to the following equation by applying Fourier transform on it.

$$G_{yy}(\omega) = H(\omega) G_{xx}(\omega) \tag{4}$$

where $G_{xx}(\omega)$ and $G_{yy}(\omega)$ are PSD matrixes of the input and output signals respectively, which can be achieved by Eqs. (5) and (6).

$$G_{xx}(\omega) = \int_{-\infty}^{\infty} R_{xx}(\tau) e^{-i\omega t} d\tau \tag{5}$$

$$G_{yy}(\omega) = \int_{-\infty}^{\infty} R_{yy}(\tau) e^{-i\omega t} d\tau \tag{6}$$

Finally, the FRF can be obtained by Eq. (7).

$$H(\omega) = \frac{G_{yy}(\omega)}{G_{xx}(\omega)} \tag{7}$$

This relation plays a key role in most of EMA methods. After obtaining the FRFs, various methods can be used to estimate the modal parameters; in this essay, the rational fraction polynomial method (RFP) [33] is employed and the natural frequencies and the mode shapes of the system are extracted, which are presented in the following sections.

Unlike the process of EMA, in the process of OMA, only the measured output response signals can be used to extract the modal parameters. The procedure of nonparametric methods of OMA which are based on the SVD algorithm is as follows [29]:

1. Measuring the output response signals.
2. Calculating the PSD of the response signals.
3. Applying the SVD on the response PSD.
4. Extracting the mode shapes and natural frequencies.

As mentioned in the introduction, if the excitation force has the characteristics similar to the white Gaussian noise, the excitation PSD will be in the form of $G_{xx}(\omega)=C[I]$, accordingly, it can be proved that just some limited modes participate in the response at each frequency. Around the natural frequencies, only one mode plays a role in the response of the system, therefore, the response at this frequency will be very similar to the mode shape of the related frequency.

Based on mentioned points, the response PSD matrix G_{yy} in Eq. (4) can be decomposed to its singular vectors and singular values matrices at each frequency by using the SVD method, which is expressed in Eq. (8):

$$\left[G_{yy}(\omega)\right]=[U][S][U]^T \tag{8}$$

In this equation, [*U*] and [*S*] are the singular vectors matrix, and the singular values matrix of the system respectively. If $\left[G_{yy}(\omega)\right]$ is *m*×*n* matrix we have:

$$[U]=\left[\{u_1\}\ \{u_2\}\ \{u_3\}\ \cdots\ \{u_r\}\right] \tag{9}$$

$$[S]=diag(s_1,.....,s_r)=\begin{bmatrix} s_1 & 0 & 0 & \cdots & 0 \\ 0 & s_2 & 0 & \cdots & 0 \\ 0 & 0 & s_3 & \cdots & 0 \\ \vdots & \vdots & & \ddots & \vdots \\ 0 & 0 & 0 & \cdots & s_r \end{bmatrix} \tag{10}$$

where

$$r=\min(m,n) \tag{11}$$

According to the relation between the singular values of the response PSD matrix and the vibrational modes of the system, the number of nonzero singular values indicates the number of vibrational modes. The frequency of the maximum singular values indicates the natural frequencies of the system, and the singular vectors corresponding to the maximum peaks of the first singular values achieve the estimation of mode shapes [34].

4 EXPERIMENTAL MODAL ANALYSIS OF THE BEAM

In order to investigate and verify the results of the numerical model by experimental tests, a cantilever beam is used which is inspired by the tailplane. In vibration analysis of the tails and wings of an aircraft, they can be taken as cantilever beams which are fixed at the base and does not experience any deflection in three directions of the coordinate system. To simulate the physical behavior of the tailplane with a beam, some prerequisites must be observed; therefore, the assumptions for modeling the tailplane with a beam are as follows: [35, 36]

1. The aspect ratio of the tailplane must be high enough to be able to express the deflection of the tailplane as one variable function.
2. The elastic axis of the tailplane must be straight to avoid coupling between the bending and torsional modes.

3. The ratio of thickness to chord in the cross-section of tailplane must be small to avoid bending in the direction of the chord.

The above-mentioned requirements have been investigated and ensured that there is the possibility to simplify the tailplane to a cantilever beam, therefore, in this study an aluminum beam with the rectangular cross-section is used to carry out the experimental tests, which is anchored at one end by rigid components (see Fig. 3). In order to stimulate the beam in EMA test, a shaker is used to apply a random force with regard to the aforementioned requisites in material and methods section; the response of the beam is measured by three accelerometers which are installed to the beam.

On the other side, in order to extract the modal parameters of the system by OMA method, one can use natural and environmental excitations, but in order to investigate the effects of noise in a controlled manner, and to be able to compare the results of EMA and OMA in the same condition, the artificial excitation namely the shaker with the random force is used. The sampling frequency of the applied random force is 2000 *Hz* with regard to the Ref. [12] for extracting the modal parameters in the frequency range of 0-1000 *Hz*. The hardware equipment of tests setup consists of *B&K* 48 *N* electromagnetic shaker model 4809, *B&K* piezo-electric accelerometer 100 *mV/g* sensitivity model 4508, *B&K* data acquisition model 3560*C*, *B&K* amplifier model 2706, anti-noise transfer cables. The setup of the laboratory beam for modal tests is presented in Fig. 3.

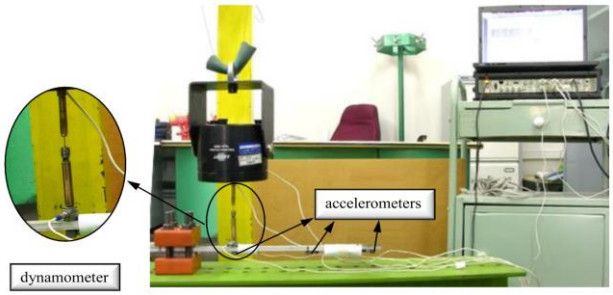

Fig.3
Setup of the beam for modal test.

4.1 Modal parameters extraction

By applying auto spectral density and cross spectral density on the acquired data in the frequency domain, the FRFs will be obtained with regard to the mentioned points in the material and methods section. The diagrams of FRFs related to three accelerometers are depicted in Fig. 4(a). As previously mentioned, the modal parameters are extracted by the RFP method [33] through the acquired FRFs (see Table 3). In the next step, the modal parameters are achieved by employing the SVD algorithm using the output data. As previously noted, the singular values and singular vectors of the PSDs should be obtained with this technique. The diagrams of singular values are depicted in Fig. 4(b); the peaks of these diagrams indicate the natural frequencies of the system. It should be noted that in this figure each line corresponds to each accelerometer's data. In the next section, the mode shapes of the system which are estimated by the singular vectors of PSD are presented.

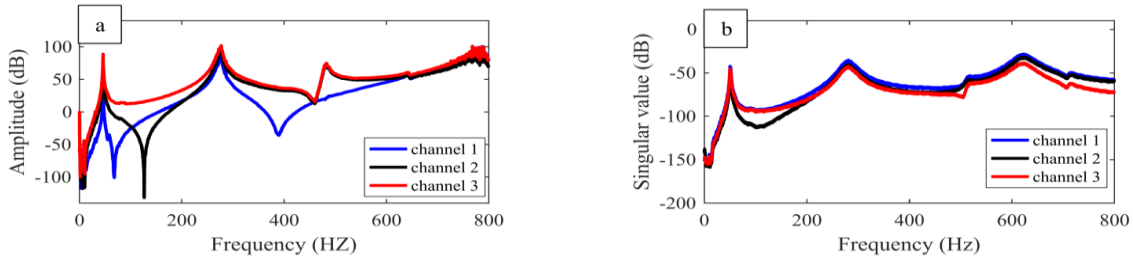

(a) (b)

Fig.4
a) Diagrams of FRFs achieved by EMA method b) Diagrams of singular values of the response PSD matrix.

The obtained natural frequencies of the beam presented in Table 3.

Table 3
Obtained natural frequencies for the beam.

Mode Shape	Analytical	EMA	OMA
First mode	44.12	46.08	50
Second mode	278.39	277	278
Third mode	778	640	621

4.2 Comparison of results

In this section, the natural frequencies and the mode shapes which were presented in previous section are compared with each other. The errors of natural frequencies which obtained experimentally versus the analytical method are presented in Table 4.

Table 4
Errors of the natural frequencies versus the analytical method (in percent).

Mode Shape	EMA	OMA	Scaled tail
First mode	4.44	13.13	47.55
Second mode	0.5	0.14	5.5
Third mode	17.7	20.17	7.43
Average	7.54	11.14	20.16

By considering the errors of the test's results, it can be seen that the average percentage of errors in the OMA method is greater than the EMA method.

According to the results which were obtained for the beam and the scaled tailplane, it can be observed that the results of scaled tailplane by the numerical method are at an acceptable level and the numerical model of the tailplane is validated. On the other side, in order to compare the mode shapes which are obtained by analytical and experimental methods, the modal assurance criterion (MAC) is used, which is defined by Eq. (12).

$$MAC(i,j)=\frac{\left|\{\phi\}^{T}_{Analytical\_i}\{\phi\}_{Experimental\_j}\right|^{2}}{\left|\{\phi\}^{T}_{Analytical\_i}\{\phi\}_{Analytical\_i}\right|\times\left|\{\phi\}^{T}_{Experimental\_j}\{\phi\}_{Experimental\_j}\right|} \tag{12}$$

where $\{\phi\}_{Analytical\_i}$ is the *ith* analytical mode shape, and $\{\phi\}_{Experimental\_j}$ is the *jth* experimental mode shape.

MAC values represent the cosine of the angle between the mode shape vectors, which means if this value equals 1, the compared mode shapes are completely similar, but if the result equals 0, there is not any similarity between them [37]; therefore, the MAC values are calculated for two groups of analytical and experimental mode shapes pairwise such that the results of OMA and EMA methods are compared with the analytical method; the results are depicted in Fig. 5.

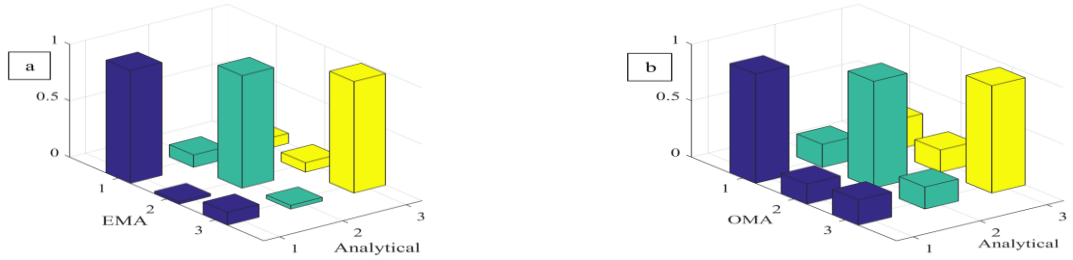

(a) (b)

Fig.5
Comparison of the two sets of estimated mode shapes by employing the MAC indicator a. analytical method and EMA method b. analytical method and OMA method.

As it can be seen in Fig. 5, the diagonal values are approximately 1, and the other values are less than 0.3, which are at an acceptable level, furthermore, the average of MAC values are presented in Table 5., which indicate that the

mode shapes which are estimated by EMA method are more accurate than those which are estimated by OMA method.

Table 5
The average of MAC values in different conditions without any noise.

Mode Shape	EMA	OMA
Diagonal values	0.987	0.9555
Non-Diagonal values	0.074	0.209

4.3 Noise effects on modal parameters

In practice, based on the quality of the setup or environmental conditions, the data of the tests contain some noise, so the input excitation or output response signals or both of them may be noisy; accordingly, the effects of noisy signals on the results is investigated in the following sections. For this purpose, firstly, it is described how to deal with this problem theoretically, and then 15% random noise is produced by coding and it is added to the input and output signals at each step by using Eq. (13).

$$N_S = S_g * \left(1 + C * N\right) \tag{13}$$

where N_S is the noisy input or output signal, S_g is the input or output signal without any noise, C is the noise coefficient and N is the noise signal.

4.4 EMA method by noisy data

For the case of noisy output, it is assumed that there is not any noise in the input, and the noise in output has not any correlation with input, then the response will consist of the genuine response with regard to the force inputs and the noise as [1]:

$$\left\{y\left(\omega\right)\right\}_{L\times 1} = \left[H\left(\omega\right)\right]_{L\times P}\left\{x\left(\omega\right)\right\}_{P\times 1} + \left\{N\left(\omega\right)\right\}_{L\times 1} \tag{14}$$

where $y\left(\omega\right)$ is the response of the system, $x\left(\omega\right)$ is the exciting force, $H\left(\omega\right)$ is the FRF, $N\left(\omega\right)$ is the noise in output, L is the number of response points and P is the number of excitation points.

Multiplying both sides of the Eq. (14) by $\left\{x\left(\omega\right)\right\}^H$, which is the Hermitian transpose of the exciting force vector, results in the estimation of the FRF matrix:

$$\left[H_1\left(\omega\right)\right]_{L\times P} = \left[G_{yx}\left(\omega\right)\right]_{L\times P}\left[G_{xx}\left(\omega\right)\right]_{P\times P}^{-1} \tag{15}$$

Based on the above theory, 15% random noise is added to the output signal, then the analysis of EMA method is performed again and the FRFs are extracted. In Fig. 6(a) the diagrams of FRFs related to three accelerometers are depicted. The obtained natural frequencies are presented in the following sections.

For the case of noisy input, similar to the previous section, it is assumed that there is not any noise in output, and the noise in input has not any correlation with the output. The input and output spectra follow:

$$\left\{y\left(\omega\right)\right\}_{L\times 1} = \left[H\left(\omega\right)\right]_{L\times P}\left\{x\left(\omega\right)\right\}_{P\times 1} - \left\{M\left(\omega\right)\right\}_{L\times 1} \tag{16}$$

where $M\left(\omega\right)$ is the noise in the input. Multiplying both sides of the Eq. (16) by $\left[y\left(\omega\right)\right]^H$, which is the Hermitian transpose of the response, results in:

$$\left[G_{yy}\left(\omega\right)\right]_{L\times L} = \left[H\left(\omega\right)\right]_{L\times P}\left[G_{xy}\left(\omega\right)\right]_{P\times L} \tag{17}$$

which yields the new estimate of the FRF matrix as:

$$\left[H_2(\omega)\right]_{L\times P} = \left[G_{yy}(\omega)\right]_{L\times L}\left[G_{xy}(\omega)\right]^{-1}_{P\times L} \tag{18}$$

This solution is correct, only when the inverse of $G_{xy}(\omega)$ exists. When the number of excitation points (P) is less than the response points (L), the inverse of $G_{xy}(\omega)$ does not exist. A pseudo-inverse has to be used to derive the FRF matrix.

Just like the previous step, 15% random noise is added to the input signal, then the analysis of EMA method is performed again and the FRFs are extracted. In Fig.6(b) the diagrams of FRFs related to three accelerometers are depicted. The obtained natural frequencies are presented in the following sections.

In the worst case, if both input and output signals are noisy, the reasonable way to find the estimate of FRF is the geometrical average of $[H_1(\omega)]$ and $[H_2(\omega)]$, which can be defined as:

$$H_3(\omega) = \sqrt{H_1(\omega)H_2(\omega)} = \sqrt{\frac{G_{yy}(\omega)}{G_{xx}(\omega)}} \tag{19}$$

For investigating the noise effects in this condition, after adding 15% random noise to the input and output signals, the diagrams of FRFs are extracted. In Fig. 6(c) the diagrams of FRFs related to three accelerometers are depicted. The obtained natural frequencies are presented in the following sections.

4.5 OMA method by noisy data

The only condition that should be investigated in the OMA method is the effects of noisy output on modal parameters identification. Just like the previous section, 15% random noise is added to the output signal and then the diagrams of singular values is extracted, which are depicted in Fig. 6(d).

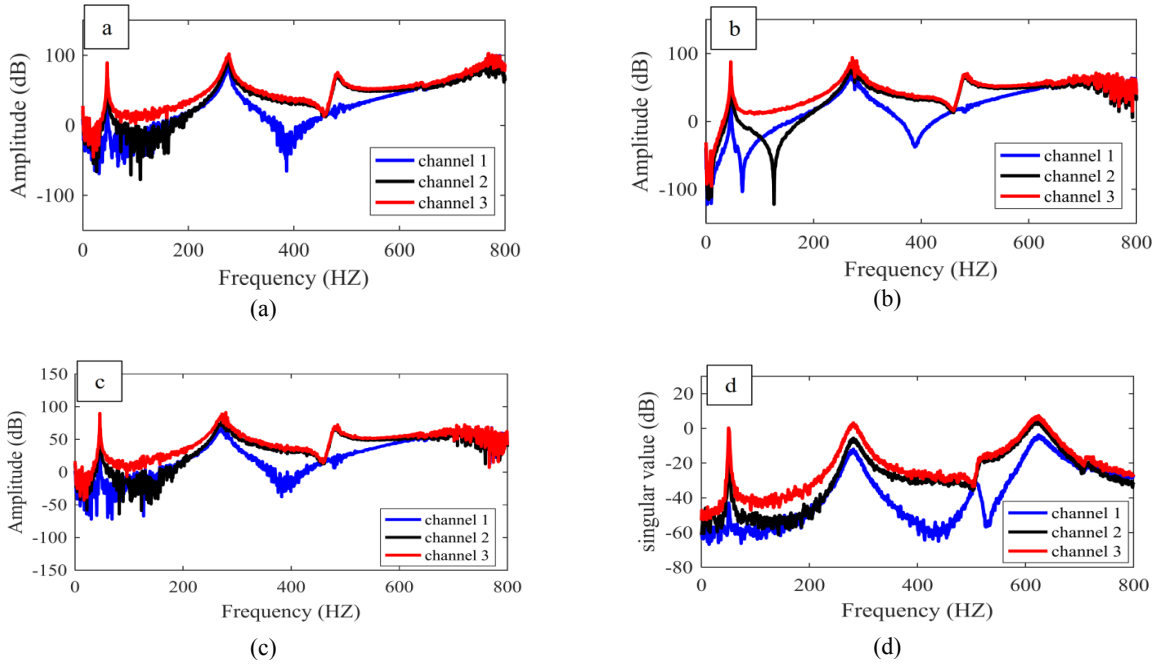

Fig.6
Diagrams of noisy data in frequency domain a. FRFs achieved by EMA method in the case of noisy output b. FRFs achieved by EMA method in the case of noisy input. c. FRFs achieved by EMA method in the case of noisy input and output d. singular values in the case of noisy output.

The natural frequencies which are obtained from EMA and OMA methods with noisy data in different conditions are listed in Table 6.

Table 6
Natural frequencies obtained from EMA and OMA modal analysis methods with noisy data.

Mode Shape	EMA by the noisy input	EMA by the noisy output	EMA by the noisy input & output	OMA by the noisy output
First mode	46	46.08	47.08	50.25
Second mode	277	277	270.8	279
Third mode	642	641.5	632.1	621

It is observed that adding noise in the measurement data results in the reduction of the accuracy of estimated natural frequencies. For further investigation, the increasing of errors in the estimated natural frequencies values with noisy data is evaluated in different conditions. The results are presented in Table 7.

Table 7
The error values of natural frequencies estimated by noisy data in different conditions (in percent).

Mode Shape	EMA by the noisy input	EMA by the noisy output	EMA by the noisy input & output	OMA by the noisy output
First mode	4.26	4.44	6.7	13.9
Second mode	0.5	0.5	8	0.2
Third mode	17.48	17.48	18.75	20.17
Average	7.41	7.47	11.15	11.42

Investigating and comparing of calculated errors in different conditions of measurement noise with respect to the values of Table 4., demonstrates that the error values in EMA by noisy input and EMA by noisy output is negligible, but in the case of EMA by noisy input and output, the average error increases about 4%; on the other side, the increasing of errors in OMA by noisy output is inconsiderable. The comparison of the mode shapes by MAC indicator are presented in Fig. 7.

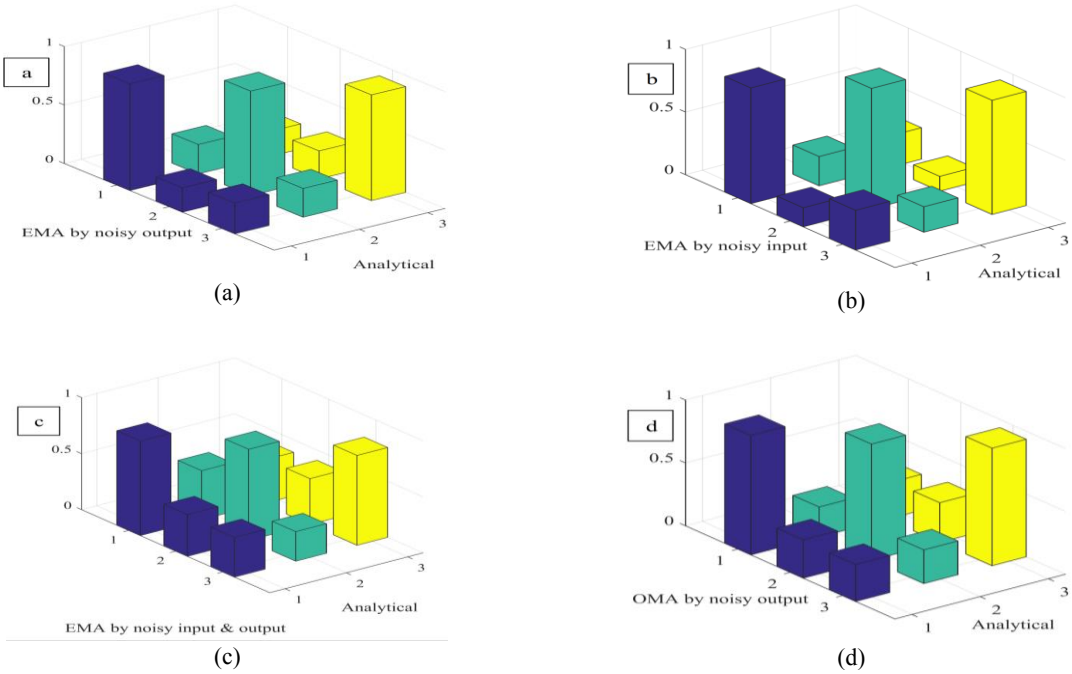

Fig.7
Comparison of the two sets of estimated mode shapes by employing the MAC indicator a. analytical method and the EMA method by noisy output b. analytical method and the EMA method by noisy input c. analytical method and the EMA method by noisy input and output d. analytical method and OMA method by the noisy output.

By analyzing the average of MAC values which are presented in Table 8., it is observed that the accuracy of mode shapes which are obtained by EMA method with noisy input and output reduced considerably, whereas in the case of OMA method by noisy output, the mode shapes affected far fewer. Therefore, it can be concluded that if a system is tested in a high noise environment, using the OMA method will lead into the more accurate results.

Table 8
The average values of the MAC estimated by noisy data in different conditions.

Mode Shape	EMA by the noisy input	EMA by the noisy output	EMA by the noisy input & output	OMA by the noisy output
Diagonal values	0.9124	0.902	0.8664	0.8964
Non-Diagonal values	0.2127	0.237	0.37	0.284

5 CONCLUSIONS

In this study, the effects of measurement noise on the process of modal parameters identification of the horizontal tailplane of aircraft using the singular value decomposition algorithm were investigated, and the findings were:

a) Increase rate of errors of obtained natural frequencies by OMA method was less than EMA method.
b) The obtained MAC values by EMA method, in the condition of noise existence in output data, were worse than the noise existence in input data, while the noise effects were almost negligible on obtained natural frequencies, in associated conditions.
c) The average of MAC values in general condition of EMA method by noisy input & output data was worse than the OMA method.

REFERENCES

[1] Fu Z.F., He J., 2001, *Modal Analysis*, Elsevier.
[2] Safarabadi M., Mohammadi M., Farajpour A., Goodarzi M., 2015, Effect of surface energy on the vibration analysis of rotating nanobeam, *Journal of Solid Mechanics* **7**(3): 299-311.
[3] Mohammadi M., Farajpour A., Goodarzi M., Mohammadi H., 2013, Temperature effect on vibration analysis of annular graphene sheet embedded on visco-Pasternak foundation, *Journal of Solid Mechanics* **5**(3): 305-323.
[4] Goodarzi M., Mohammadi M., Farajpour A., Khooran M., 2014, Investigation of the effect of pre-stressed on vibration frequency of rectangular nanoplate based on a visco-Pasternak foundation, *Journal of Solid Mechanics* **6**(1): 98-121.
[5] Goodarzi M., Mohammadi M., Khooran M., Saadi F., 2016, Thermo-mechanical vibration analysis of FG circular and annular nanoplate based on the visco-pasternak foundation, *Journal of Solid Mechanics* **8**(4): 788-805.
[6] Arda M., Aydogdu M., 2018, Longitudinal magnetic field effect on torsional vibration of carbon nanotubes, *Journal of Computational Applied Mechanics* **49**(2): 304-313.
[7] Hosseini M., Hadi A., Malekshahi A., Shishesaz M., 2018, A review of size-dependent elasticity for nanostructures, *Journal of Computational Applied Mechanics* **49**(1): 197-211.
[8] Goodarzi M., Bahrami M.N., Tavaf V., 2017, Refined plate theory for free vibration analysis of FG nanoplates using the nonlocal continuum plate model, *Journal of Computational Applied Mechanics* **48**(1): 123-136.
[9] Zargaripoor A., Daneshmehr A., Isaac Hosseini I., Rajabpoor A., 2018, Free vibration analysis of nanoplates made of functionally graded materials based on nonlocal elasticity theory using finite element method, *Journal of Computational Applied Mechanics* **49**(1): 86-101.
[10] Lau J., Debille J., Peeters B., Giclais S., Lubrina P., Boeswald M., Govers Y., 2011, Advanced systems and services for ground vibration testing—application for research test on an Airbus A340-600 Aircraft, *15th International Forum on Aeroelasticity and Structgural Dynamics,* Paris, France.
[11] Neu E., Janser F., Khatibi A.A., Orifici A.C., 2015, Operational modal analysis of a cantilever in a wind tunnel using optical fiber bragg grating sensors, *Proceedings of the 6th International Operational Modal Analysis Conference,* Gijón, Spain.
[12] Neu E., Janser F., Khatibi A.A., Braun C., Orifici A.C., 2016, Operational modal analysis of a wing excited by transonic flow, *Aerospace Science and Technology* **49**: 73-79.
[13] Neu E., Janser F., Khatibi A.A., Orifici A.C., 2017, Fully automated operational modal analysis using multi-stage clustering, *Mechanical Systems and Signal Processing* **84**: 308-323.
[14] Jelicic G., Schwochow J., Govers Y., Sinske J., Buchbach R., Springer J., 2017, Online monitoring of aircraft modal parameters during flight test based on permanent output-only modal analysis, *58th AIAA/ASCE/AHS/ASC Structures, Structural Dynamics, and Materials Conference*.

[15] Jia P., Lai S.K., Zhang W., Lim C.W., 2014, Experimental and FEM modal analysis of a deployable-retractable wing, *Modern Mechanical Engineering* **4**(04):183.
[16] Moaveni B., Barbosa A.R., Conte J.P., Hemez F.M., 2014, Uncertainty analysis of system identification results obtained for a seven story building slice tested on the UCSDNEES shake table, *Structural Control and Health Monitoring* **21**(4): 466-483.
[17] Mellinger P., Döhler M., Mevel L., 2016, Variance estimation of modal parameters from output-only and input/output subspace-based system identification, *Journal of Sound and Vibration* **379**: 1-27.
[18] Pintelon R., Schoukens J., 1990, Robust identification of transfer functions in the s-and z-domains, *IEEE Transactions on Instrumentation and Measurement* **39**(4): 565-573.
[19] Gu G., Misra P.R.A.D.E.E.P., 1992, Identification of linear time-invariant systems from frequency-response data corrupted by bounded noise, *IEE Proceedings D-Control Theory and Applications* **139**(2): 135-140.
[20] Bai E.W., Raman S., 1993, A linear interpolatory algorithm for robust system identification with corrupted measurement data, *IEEE Transactions on Automatic Control* **38**(8): 1236-1241.
[21] Pintelon R., Guillaume P., Schoukens J., 1996, Measurement of noise (cross-) power spectra for frequency-domain system identification purposes: large-sample results, *IEEE Transactions on Instrumentation and Measurement* **45**(1):12-21.
[22] Schoukens J., Pintelon R., 2006, Estimation of nonparametric noise models, *Instrumentation and Measurement Technology Conference.*
[23] Schoukens J., Pintelon R., Rolain Y., 2004, Box–Jenkins alike identification using nonparametric noise models, *Automatica* **40**(12): 2083-2089.
[24] Schoukens J., Rolain Y., Pintelon R., 2010, On the use of parametric and non-parametric noise-models in time-and frequency domain system identification, *Decision and Control (CDC).*
[25] Juang J.N., Pappa R.S., 1986, Effects of noise on modal parameters identified by the eigensystem realization algorithm, *Journal of Guidance, Control, and Dynamics* **9**(3): 294-303.
[26] Li P., Hu S.L.J., Li H.J., 2011, Noise issues of modal identification using eigensystem realization algorithm, *Procedia Engineering* **14**:1681-1689.
[27] Dorvash S., Pakzad S.N., 2012, Effects of measurement noise on modal parameter identification, *Smart Materials and Structures* **21**(6): 065008.
[28] Brincker R., Zhang L., Andersen P., 2000, Modal identification from ambient responses using frequency domain decomposition, *18th International Modal Analysis Conference (IMAC),* San Antonio, Texas.
[29] Brincker R., Zhang L., Andersen P., 2001, Modal identification of output-only systems using frequency domain decomposition, *Smart Materials and Structures* **10**(3): 441.
[30] Ayari F., Bayraktar E., 2011, Parametric study to optimize aluminum shell structure under various conditions, *Experimental and Applied Mechanics,* **6**: 439-450.
[31] Ewins D.J., 1984, *Modal Testing: Theory and Practice*, Letchworth, Research Studies Press.
[32] Rahman A.G.A., Ong Z.C., Ismail Z., 2011, Enhancement of coherence functions using time signals in modal analysis, *Measurement* **44**(10): 2112-2123.
[33] Richardson M.H., Formenti D.L., 1982, Parameter estimation from frequency response measurements using rational fraction polynomials, *Proceedings of the 1st International Modal Analysis Conference*, Union College Schenectady.
[34] Brincker R., Ventura C., Andersen P., 2001, Damping estimation by frequency domain decomposition, *19th International Modal Analysis Conference.*
[35] Haddadpour H., Firouz-Abadi R.D., 2006, Evaluation of quasi-steady aerodynamic modeling for flutter prediction of aircraft wings in incompressible flow, *Thin-Walled Structures* **44**(9): 931-936.
[36] Moosavi M.R., Oskouei A.N., Khelil A., 2005, Flutter of subsonic wing, *Thin-Walled Structures* **43**(4): 617-627.
[37] Allemang R.J., Brown D.L., 1982, A correlation coefficient for modal vector analysis, *Proceedings of the 1st International Modal Analysis Conference,* SEM Orlando.